ACS SENSORS

pubs.acs.org/acssensors Article

# Rapid Detection of *Pseudomonas aeruginosa* Biofilms via Enzymatic Liquefaction of Respiratory Samples

Antonio Clemente,* Alejandra Alba-Patiño, Estrella Rojo-Molinero, Steven M. Russell, Marcio Borges, Antonio Oliver, and Roberto de la Rica*

Cite This: https://dx.doi.org/10.1021/acssensors.0c01618 Read Online

ACCESS | Metrics & More | Article Recommendations | Supporting Information

**ABSTRACT:** Respiratory infections caused by multi-drug-resistant *Pseudomonas aeruginosa* often yield poor outcomes if not detected right away. However, detecting this pathogen in respiratory samples with a rapid diagnostic test is challenging because the protective biofilms created by the pathogen are themselves surrounded by a high-viscosity sputum matrix. Here, we introduce a method for liquefying respiratory samples and disrupting bacterial biofilms on the spot within a minute. It relies on the generation of oxygen bubbles by bacterial catalase through the addition of hydrogen peroxide. When coupled with a mobile biosensor made of paper, the resulting diagnostic kit was able to detect *P. aeruginosa* infections in sputa from patients with excellent sensitivity and specificity within 8 min. The quick turnaround time along with few infrastructure requirements make this method ideal for the rapid screening of *P. aeruginosa* infections at the point of care.

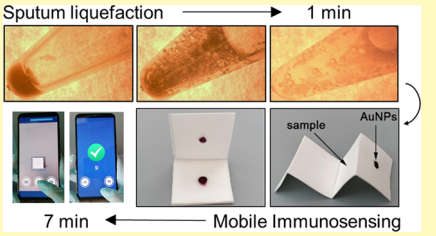


**KEYWORDS:** *pathogen, sputum, bacteria, catalase, biosensor, immunosensor, smartphone, colorimetric*



Unattended infections can progress to systemic inflammation and multiorgan dysfunction (i.e., sepsis), leading to a poor prognosis and potential long-term sequelae.[1] It is known that sepsis survival rates decrease when the antimicrobial treatment is delayed.[2] Accordingly, protocols for sepsis management recommend an empiric antibiotic regime as soon as possible, and preferably within the first hour of suspecting sepsis.[3] Yet, infections caused by antibiotic-resistant pathogens still yield poor outcomes even when antibiotics are administered in a timely manner.[4] This is particularly problematic in the context of sepsis caused by *Pseudomonas aeruginosa* infections because many strains are only treatable with one antibiotic: colistin. Colistin is rather toxic when administered intravenously and not routinely recommended within the first empirical antibiotic regime.[5] In this situation, patients can rapidly progress to deadly septic shock. Pathogen identification through bacteriological culture takes too long to guide the first antibiotic treatment. Multi-drug-resistant *P. aeruginosa* is highly prevalent in hospital-acquired pneumonia, and pneumonia is the underlying infection in 45% of sepsis cases in the US and Europe.[6] Thus, there is a specific need to develop technologies for the rapid detection of *P. aeruginosa* in respiratory samples. Such a test would alert clinicians to infections by this hazardous pathogen, thus providing much-needed guidance during the administration of the first antibiotic regime.

Using a rapid biosensor could tackle this issue by revealing the presence of *P. aeruginosa* in respiratory samples at the point of care.[7−13] Paper-based immunosensors would be ideal candidates for this application since they can be disposed of by incineration, thus destroying any hazardous respiratory pathogens. However, detecting *P. aeruginosa* in respiratory samples such as sputum and bronchial aspirate with immunosensors is challenging due to the barriers surrounding the pathogen. First of all, the sample matrix is made of highly cross-linked mucins with a highly viscous or even semisolid consistency.[14] Pathogens trapped within this matrix are not readily available for detection. Second, within this matrix, *P. aeruginosa* further encases itself in a biofilm.[15,16] Bacteria trapped within the biofilm are also not detectable. Thus, the detection of *P. aeruginosa* in these samples requires the liquefaction and homogenization of samples as well as the rupture of bacterial biofilms to avoid false negatives. Current approaches for processing respiratory samples are cumbersome and often require infrastructures such as a vortex, an incubator, or a particle manipulator.[17−22] Furthermore, it has not been proven that these methods disrupt biofilms. A method that instantly liquefies respiratory samples and also disrupts biofilms could enable the detection of respiratory pathogens at the point of care. This would enable a personalized approach for administering the first antibiotic regime since nosocomial infections by this pathogen require a different therapeutic approach than the rest.

**Received:** August 5, 2020
**Accepted:** November 12, 2020

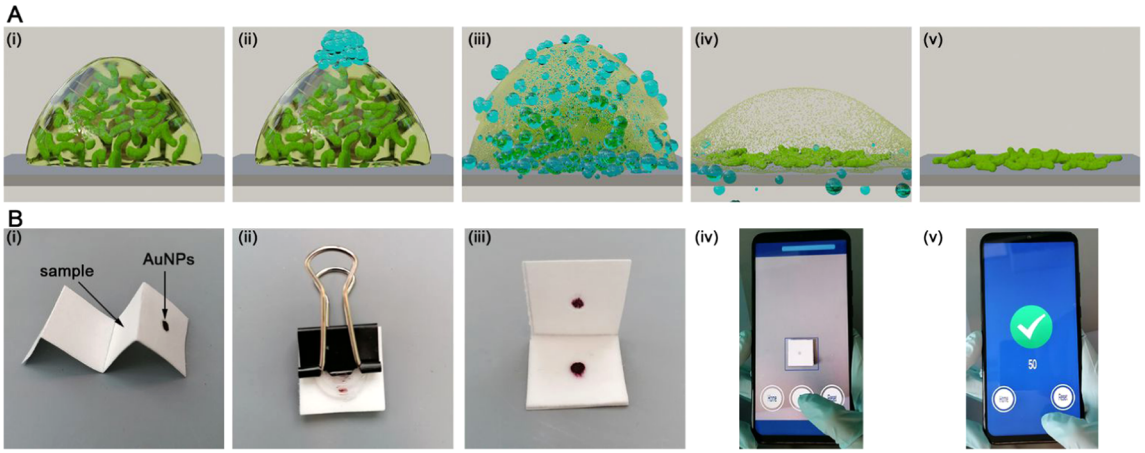


**Figure 1.** Schematic representation of sample liquefaction (A) and *P. aeruginosa* detection (B) with the proposed method. (A) Bacteria are trapped in biofilms within respiratory samples (i) and the addition of $H_2O_2$ (ii) causes catalase enzymes to generate oxygen bubbles (iii), which liquefy the sample and destroy biofilms in one step (iv, v). (B) Origami immunosensors consist of a piece of paper folded into four 2 cm × 2 cm squares (i); the top square contains a nanoparticle reservoir.[32] After adding the sample, the immunosensor is folded and the nanoparticles are transferred to the detection area (ii); after washing away excess reagents, the recognition of bacterial antigens by antibody-decorated gold nanoparticles generates a colored spot (iii); and the spot is detected and quantified by aligning the paper biosensor with a smartphone app (iv) and pressing a button (v).

In this paper, we describe a new approach for disrupting *P. aeruginosa* biofilms and liquefying sputum samples in one step. It only requires adding an aqueous solution of hydrogen peroxide to the sample. Bacterial catalase enzymes generate oxygen bubbles that break the biofilm and liquefy the sample matrix within a minute (Figure 1A). No additional instrumentation or separation steps are required. Catalase has been previously used as an enzyme label or biorecognition element in biosensing,[23−25] and as a building block for micro/nanomotors,[26−28] biofuel cells,[29] and drugs.[30] Here, we introduce a novel use of this enzyme for liquefying respiratory samples prior to immunodetection. Catalase is produced by *P. aeruginosa*, as well as by staphylococci, and *Enterobacteriaceae*, which also generate biofilms and are highly prevalent in patients with hospital-acquired pneumonia.[6] It is also present in other bacterial and fungal species, making this approach useful for dissolving respiratory samples for a wide array of pathogens. Once the pathogens have been released from the matrix and their biofilms, they are available to be detected with a rapid diagnostic test at the point of care. Here, we demonstrate this concept using paper immunosensors with a mobile readout (Figure 1B). In these devices, a drop of liquefied sample is applied to a paper substrate and dried for 30 s (Figure 1B(i)). This step traps bacterial antigens in the cellulose matrix. Next, the paper is folded to transfer antibody-decorated gold nanoparticles from a reservoir to the detection zone for 5 min (Figure 1B(ii)). The specific recognition of *P. aeruginosa* antigens attached to the paper generates a colored spot (Figure 1B(iii)), which is then quantified with a smartphone app in a matter of seconds (Figure 1B(iv, v)).[31] The whole process, including sample liquefaction and pathogen detection, can be performed in less than 8 min by a frontline healthcare worker. This quick turnaround time makes our detection kit suitable for guiding antibiotic prescriptions at the point of care, a much-needed development for improving sepsis management.

## MATERIALS AND METHODS

**Liquefaction of Sputum Samples.** Sputum samples were collected by the Microbiology Unit at Son Espases University Hospital (Balearic Islands). Quantitative culture for bacterial pathogens was carried out by plate counting of bacterial colonies after seeding serial dilutions of sputum previously homogenized with Sputasol (6.5 mM dithiotreitol). Samples with a bacterial load $\geq 10^5$ colony-forming units (cfu) were considered respiratory tract infections. Sputum samples negative for bacterial infection, determined using Gram's stain screening test, were included as controls.

Prior to liquefaction, raw samples containing *Pseudomonas aeruginosa* (PA+), *Staphylococcus* spp., or different species of the *Enterobacteriaceae* family (PA−) as infection-causing pathogens or a mixed flora (MF) were collected and kept at −20 °C until used. After thawing at room temperature (RT), 10 mg was collected in a 1.5 mL Eppendorf tube and liquefied by adding 0.3 M $H_2O_2$ in PBS at a constant 20:1 ratio (v/w) for 60 s. To demonstrate that sputum liquefaction is due to the oxygen bubbles produced by catalase, enzymes in the PA+ and MF sputum samples were inhibited by adding 100 μL $NaN_3$ at different concentrations for 2 h at RT. Then, the solution was carefully removed and 0.3 M $H_2O_2$ was added. Videos and photographs were obtained using a LEICA MC170 HD digital camera coupled to a ZuZi stereo microscope with transmitted illumination.

***In Vitro* Disruption of *P. aeruginosa* Biofilms.** *Pseudomonas aeruginosa* (PA) biofilms were obtained by a closed system in 96-well, round-bottom microtiter plates. Plates were filled with 100 μL sterile Luria−Bertani (LB) broth culture and inoculated with the PAO1 strain. After 24 h of incubation in a 5% $CO_2$ atmosphere and at 37 °C, biofilm formation occurred as a ring around the well. To carry out studies of PA biofilms by confocal laser scanning microscopy (CLSM), we followed a previously published protocol, with some modifications.[33] Briefly, eight-well microslide ibiTreat chambers (ibidi) were filled with 300 μL LB, inoculated with the PAO1 strain, and incubated in a 5% $CO_2$ atmosphere and at 37 °C for 24−48 h in a closed system.

To study the effect of $H_2O_2$ in the biofilm microstructure, the LB broth culture was carefully removed from plates after biofilm formation and then the wells were gently rinsed, keeping flocs untouched, by repeatedly filling and emptying with PBS (final volume of 100 μL per well). Finally, 50 μL PBS containing increasing amounts of $H_2O_2$ was added and incubated for 5 min. Micrographs were obtained using a Cell Observer inverted microscope (Carl Zeiss). Images were obtained in the same coordinate of each microwell before and after $H_2O_2$ treatments using 5× objective lenses with bright-field illumination. Densitometric analysis was performed with Photoshop by calculating the pixel intensity (PI) of the whole


https://dx.doi.org/10.1021/acssensors.0c01618
ACS Sens. XXXX, XXX, XXX−XXX

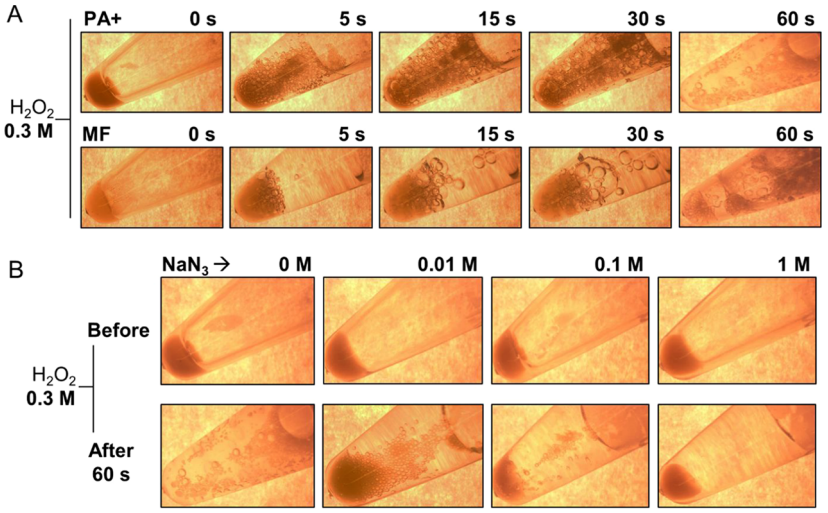


**Figure 2.** Sputum liquefaction. (A) Photographs of sputum samples (10 mg) containing *P. aeruginosa* (PA+) or a mixed flora (MF) before (0 s) and after the addition of 0.3 M $H_2O_2$ for 5, 15, 30m, or 60 s. (B) Photographs of PA+ sputum samples pretreated with different concentrations of $NaN_3$ before and 60 s after the addition of 0.3 M $H_2O_2$.

image using the histogram function with the luminosity channel. The colorimetric signal S was taken as the integer value after subtracting the background signal. The increase in the colorimetric signal (ΔS) was obtained by subtracting S measured after $H_2O_2$ treatment from S before $H_2O_2$ treatment. To evaluate with higher resolution the effect of $H_2O_2$ on the biofilm architecture, LB broth was carefully removed from microslides prepared for CLSM studies, and live cells and extracellular polymeric substances (EPS) were, respectively, stained with 17 μM SYTO9 (Invitrogen) and 100 $\mu g \cdot mL^{-1}$ concanavalin A-tetramethylrhodamine isothiocyanate (ConA-TRIC, Invitrogen) in 0.1 M sodium bicarbonate (pH 8.3).[34] CLSM images were obtained using an LSM 710 confocal microscope (Carl Zeiss) before and after $H_2O_2$ treatments using 63X oil immersion objective lenses. CLSM measurements were also made on biofilms grown under Fe starvation conditions to downmodulate catalase activity[35] (following the method shown in Figures S5 and S6).

Experiments to disrupt biofilms attached to the plates were performed as follows: first, the plates were decanted to remove all planktonic cells and flocs. They were then rinsed in three sequential steps by immersing the plate in sterile PBS, decanting, and tapping paper towels over them. Next, 175 μL PBS containing increasing concentrations of $H_2O_2$ was added for 60 s. To demonstrate the release of antigens from the biofilms attached to the plate, the supernatants after hydrogen peroxide treatment were analyzed with ELISA as explained in the Supporting Information.

The following experiments were performed to elucidate whether adding $H_2O_2$ for 60 s would kill cells and detach them from the biofilm. After following the above-mentioned biofilm disruption protocol, $H_2O_2$ was removed by immersing the plates in PBS once. Next, wells were decanted by inverting the plate and filled with 100 μL PBS. The remaining bacteria that adhered to the inner surface of the wells were gently detached by bath sonication (two cycles of 30 s at 160 W with 1 min intervals) and stained with 5 μL of 75 μM P-Io (propidium iodide, BD Pharmingen) for 15 min at RT. The plates were then centrifuged at 3000 rpm for 5 min, excess of P-Io was removed by discarding supernatants, and bacterial pellets were resuspended with 100 μL PBS. Finally, stained bacteria were pipetted into a 96-well black plate (Greiner Bio-One) and the P-Io fluorescence was measured in a Sinergy H1 microplate reader (Biotek). After autofluorescence subtraction, the percentage increase of P-Io fluorescence intensity (FI) was expressed as [(FI after $H_2O_2$ treatment—FI without $H_2O_2$ treatment)/FI without $H_2O_2$ treatment] × 100.

**Detection of *P. aeruginosa* with Origami Immunosensors.** Gold nanoparticles (AuNPs) with a diameter of 40 nm were synthesized following the Turkevich method as described previously.[32] Trisodium citrate at a final concentration of 0.75 mM was added to a boiling gold chloride hydrate solution with a concentration of 0.50 mM for 10 min on a heated plate with vigorous stirring. Nanoparticle growth was confirmed by the appearance of a dark red-wine color. When the solution reached RT, the AuNPs were consecutively pegylated, concentrated, and functionalized with avidin according to the procedure described previously.[32] Antibody-decorated nanoparticles were obtained by adding 10 μL polyclonal biotin anti-*Pseudomonas aeruginosa* developed in rabbit (Invitrogen) to 100 μL avidin-decorated nanoparticles for 1 h. Free biotin-binding sites were capped with 0.1 mM biotin−PEG (O−[2-(Biotinyl−amino)ethyl]−O′−(2-carboxyethyl)−polythylene glycol, Mw: 3.000, Sigma) for 30 min. Excess reagents were washed away by three consecutive centrifugation steps at 4 °C and 6000 rpm during 6 min using PBST as washing buffer. Origami immunosensors were fabricated as follows: Whatman paper #41 was cut into 2 cm × 8 cm strips, which were folded like an accordion to yield four 2 cm × 2 cm squares as shown in Figure 1B. The top square was modified with wax. To accomplish this, waxed paper (PME) was cut into 2 cm × 2 cm squares. A 5 mm × 5 mm circle was cut in the center using a hole puncher. The wax was transferred to the Whatman paper by pressing with a hot iron, causing the melted wax to penetrate into the paper. The procedure was repeated on the other side of the paper to completely seal it. In the circle at the center of the paper that remained unwaxed, a nanoparticle reservoir was fabricated by adding 3 μL of 30% polystyrene sulfonate (PSS, MW 700.000, Sigma) and letting it dry at RT.[32] Then, 1 μL antibody-decorated nanoparticles were added and dried at RT.

To detect *P. aeruginosa*, 10 μL of sample was spotted onto the receiving paper substrate and dried with a hair drier for 30 s. Subsequently, the paper biosensors were blocked by adding 1 mL of PBS−BSA. The paper was immediately folded to transfer antibody nanoparticles from the reservoir to the detection zone by pressing with a clamp for 5 min. Next, the reservoir was peeled off and the receiving paper was washed five times with PBST. Finally, the colorimetric signal was measured immediately afterward with a densitometry app as explained below. Bacterial suspensions in PBS containing *P. aeruginosa* (PAO1 strain) were used as samples for calibrating the immunosensors. The suitability of the proposed method for detecting pathogens in real patient samples was tested with a panel of sputum samples obtained from the Microbiology Unit at Son Espases University Hospital with approval from the local ethics committee (protocol IB 4005/19 PI).

**Densitometry App.** App development has been described elsewhere.[32] It was installed in a Huawei POT-LX1 smartphone. To quantify signals, the user aligns the square piece of paper with a virtual


https://dx.doi.org/10.1021/acssensors.0c01618
ACS Sens. XXXX, XXX, XXX−XXX

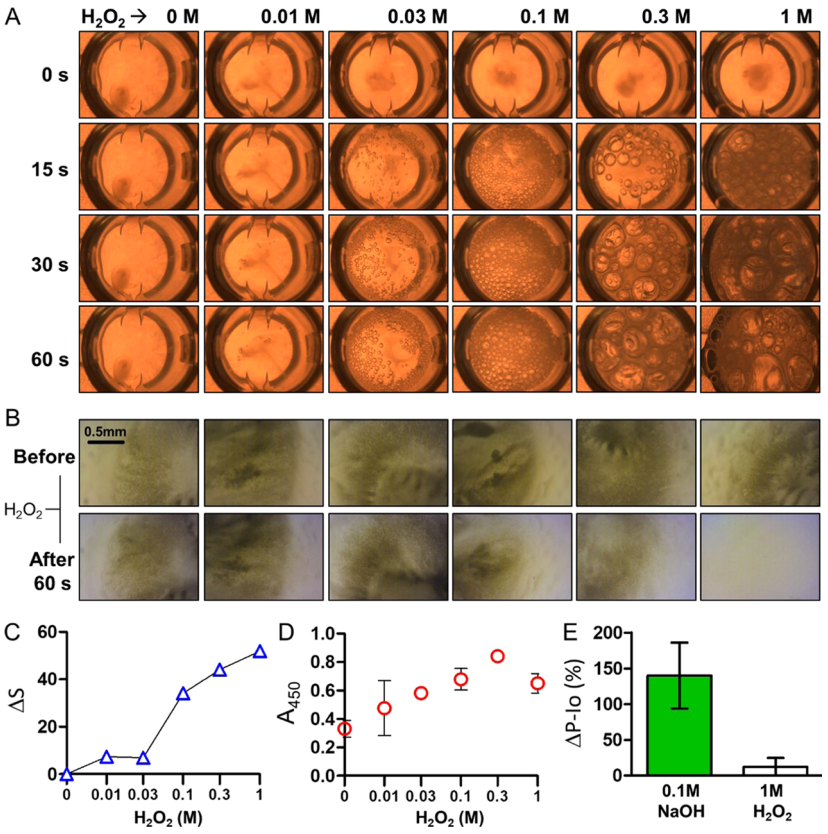


**Figure 3.** Biofilm disruption. (A) Photographs of *P. aeruginosa* biofilms grown in a 96-well plate before and after adding $H_2O_2$ at different concentrations for 0, 15, 30, and 60 s. (B) Micrographs of the biofilms before and 60 s after adding $H_2O_2$ at the concentrations shown in (A). (C) Increase in the colorimetric signal (illuminance, ΔS) calculated from micrographs in (B). (D) Detection of bacterial antigens released from biofilms attached to the plate after adding $H_2O_2$ at different concentrations for 60 s; error bars are the standard deviation ($n$ = 6). (E) Percentage increase of propidium iodide (P-Io) fluorescence intensity (cell death) after adding 1 M $H_2O_2$ (white bar) or 0.1 M NaOH (green bar) as a positive control for 60 s. Bars represent the mean value, and error bars are the standard deviation ($n$ = 5).

frame. This fixes the distance and angle of the smartphone with respect to the assay. After pressing "set," the app automatically finds the region of interest and quantifies the increase of pixel intensity with respect to the background. Compensation for different illuminance and uneven illumination conditions is calculated automatically. When the app has performed 50 valid measurements, the screen displays the average value. The process takes less than 10 s. Figure S8 shows a comparison between the app and a manual method for densitometric analysis using a scanner and image processing software ImageJ.

**Data Analysis.** Statistical analysis was performed using GraphPad Prism software. Data are expressed as mean ± standard deviation (SD) or median with the 25th and 75th percentile. The Kruskal–Wallis test was used to compare values of biomass and bacterial membrane permeability among differently treated biofilms or values of immunosensor signals among different sputum samples. A $P$ value <0.05 was considered statistically significant.

## RESULTS

Our method for the rapid detection of *P. aeruginosa* in respiratory samples is based on the generation of bubbles by the enzyme catalase, which liquefies the sample (Figure 1A). Microparticles have been previously used for mechanically disrupting sputum samples.[17] We hypothesized that oxygen bubbles could have a similar effect without using mixers to stir the sample. Since the catalase is produced by *P. aeruginosa*, and bacteria are trapped within the biofilm, we envisioned that the bubbles would not only liquefy the sputum but also disrupt the biofilm simultaneously. To study whether oxygen bubbles could liquefy sputum, 10 mg of sputum samples containing *P. aeruginosa* (PA+) or a mixed flora (MF) were introduced in an Eppendorf tube and treated with 200 μL of 0.3 M $H_2O_2$. In Video S1, PA+ samples generate bubbles that liquefy the sample within 60 s. The sample looks transparent after dispersing the bubbles (Figure 2A), which shows that it has been completely liquefied. Mixed flora samples also generate bubbles, although more slowly, which indicates that they contain fewer catalase enzymes (Video S2). Samples still contain dark spots 60 s after the addition of hydrogen peroxide, which indicates that they are not fully liquefied. To demonstrate that the bubbles are generated by catalase, the sputum containing *P. aeruginosa* was pretreated with different concentrations of a catalase inhibitor ($NaN_3$). In Videos S3–S5, samples incubated with $NaN_3$ generate fewer bubbles as the concentration of inhibitor increases.

In Figure 2B, samples appear opaque and unchanged by the addition of hydrogen peroxide when pretreated with $NaN_3$. These experiments demonstrate that the bubbles are generated by the catalase-mediated hydrolysis of $H_2O_2$. They also indicate that the main factor behind sample liquefaction is the enzymatic generation of bubbles since samples that do not generate these bubbles remain solid after the addition of hydrogen peroxide (Figure 2B, 1 M $NaN_3$).

Next, we studied whether the hydrogen peroxide treatment could disrupt the biofilms and liberate bacterial antigens. To this end, *P. aeruginosa* biofilms were grown at the bottom of a 96-well plate. After washing away excess planktonic cells while


https://dx.doi.org/10.1021/acssensors.0c01618
ACS Sens. XXXX, XXX, XXX−XXX

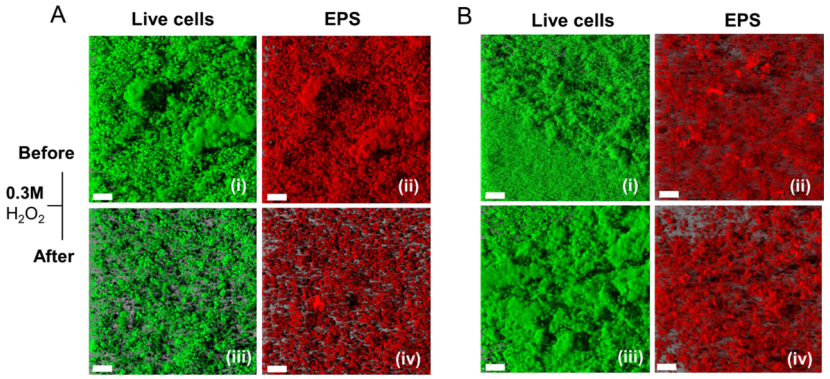


**Figure 4.** Live cells and extracellular polymeric substances in *P. aeruginosa* biofilms after $H_2O_2$ treatment. (A) Three-dimensional confocal imaging before (i, ii) and after (iii, iv) 0.3 M $H_2O_2$ treatment in control biofilms or (B) biofilms with low catalase activity grown in the presence of an Fe chelator (0.25 mM 2-2′-bipyridyl) for 48 h. Green (SYTO9) and red (ConA-TRIC) colors indicate the presence of live cells and extracellular polymeric substances (EPS), respectively. Scale bar: 15 $\mu$m.

keeping the suspended aggregates or flocs untouched, $H_2O_2$ was added at different concentrations and the generation of bubbles was recorded for 60 s (Figure 3A). Biofilm disruption was documented by taking a photograph before and after the treatment (Figure 3B). In Figure 3A, samples without $H_2O_2$ did not generate any bubbles, and micrographs of the biofilms in Figure 3B showed that they were mainly unaltered. When the concentration of $H_2O_2$ was higher than 0.01 M, samples started to effervesce. As the concentration of $H_2O_2$ increased, the amount and size of the generated bubbles also increased (Figure 3A). In Figure 3B, images look less opaque when the concentration of $H_2O_2$ increased because the biofilm flocs were being dissolved. Densitometric analysis of the images shown in Figure 3B confirmed this trend (Figure 3C).

In Figure 4A, confocal 3D images of biofilms show intense fluorescent signals and accurate colocalization of SYTO9 (green) and ConA-TRIC (red) dyes (Figure 4A(i,ii)), indicating a dense biomass encrusted in the EPS matrix. After addition of 0.3 M $H_2O_2$, both signals drastically decrease (Figure 4A(iii,iv)), which demonstrates a deep disruption of the biofilm architecture (cells and substances surrounding them). In Figure S4, confocal 3D images show that despite biofilm disruption the cell viability is conserved, confirming the fact that biofilm disruption is predominantly caused by the generation of bubbles and not by the biocide action of $H_2O_2$. To further demonstrate that the catalase-induced generation of bubbles is key for biofilm disruption, the same experiments were repeated with biofilms grown in the presence of an Fe chelator, which diminishes catalase activity and reduces the production of bubbles.[35] In Figure 4B, confocal 3D images of Fe-starved biofilms show that both green and red signals (Figure 4B(iii,iv)) are similar to those observed before the addition of $H_2O_2$ (Figure 4B(i,ii)). This means that the biofilm architecture is much less altered than that in Figure 4A, even though the cells are less protected from the biocide action of $H_2O_2$ (catalase activity is lower) and generate less EPS (the red signal is less intense than that in Figure 4A). These results demonstrate that the generation of bubbles is the main factor behind biofilm disruption induced by $H_2O_2$ (Figures 4B(i,iii) and S4) regardless of the amount of protective EPS (Figure 4B(ii−iv)).

To demonstrate that $H_2O_2$ can induce the release of bacteria from the biofilms attached to the plate, we first washed away excess planktonic cells and flocs and added $H_2O_2$ at different concentrations. Then, supernatants were collected at different times and analyzed with ELISA using the method shown in Figure S1. In Figure 3D, the ELISA signal increased as the concentration of $H_2O_2$ increased, which indicates that bacterial antigens were found at higher concentrations in the supernatants after the treatment. This further supports the hypothesis that pathogens were liberated from the biofilm due to the generation of bubbles. The ELISA signal slightly decreased when the concentration of $H_2O_2$ was 1 M, even though the biofilms seem to be completely dissolved in Figure 3B,C. Supplementary experiments showed that the addition of $H_2O_2$ interfered with antibody−antigen interactions when supplied at 1 M (Figure S2), which explained the decrease in signal seen in Figure 1D. Increasing the incubation time with $H_2O_2$ to 3 or 5 min resulted in more bacterial antigens being released from the biofilms at low concentrations of hydrogen peroxide, but the maximum signal at 0.3 M remained unaffected (Figure S3). Consequently, a $H_2O_2$ concentration of 0.3 M and an incubation time of 60 s were chosen for subsequent experiments, since these conditions completely liquefied sputum samples (Figure 2) and liberated antigens from biofilms (Figure 3D) without hampering immunodetection to a large extent (Figure S2).

Hydrogen peroxide can induce intracellular production of highly reactive hydroxyl free radicals that could compromise membrane permeability.[36] In Figure 3E, a cell viability test showed that the membrane permeability of *P. aeruginosa* cells was not affected by the addition of $H_2O_2$ with a concentration as high as 1 M when it was added for only 60 s. This indicates that the ELISA signals recorded in Figure 3D originated from biofilm disruption, which was mainly caused by the generation of bubbles, and that the biocide action of $H_2O_2$ plays a less relevant role when added at 0.3 M for only 60 s. This was also confirmed by confocal 3D imaging of biofilms after live/dead staining (Figure S4). Biofilms grown under Fe starvation conditions generated fewer bubbles and released fewer antigens upon treatment with hydrogen peroxide (Figures S5 and S6). This experiment corroborated the evidence that the production of catalase by the pathogens was the key factor behind the effervescence and antigen release shown in Figure 3.

After demonstrating the enzymatic rupture of biofilms and concomitant liquefaction of sputum samples, we sought to apply this method for the rapid detection of respiratory infection by *P. aeruginosa*. To accomplish this, we combined it with a mobile immunosensor for the rapid detection of bacteria


https://dx.doi.org/10.1021/acssensors.0c01618
ACS Sens. XXXX, XXX, XXX−XXX

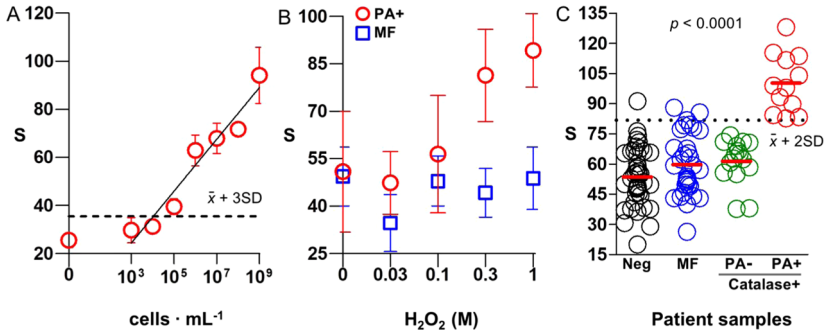


**Figure 5.** Detection of *P. aeruginosa* with the mobile immunosensors shown in Figure 1B in solutions containing bacteria at known concentrations (A), in sputum samples classified as infected by the pathogen (PA+) or containing a mixed flora (MF) after addition of $H_2O_2$ at different final concentrations (B), and in a panel of patient samples (C). Error bars are the standard deviation ($n$ = 3). $X$ is the average and SD is the standard deviation. In (A), the dotted line shows signals above three times the standard deviation of the blank. In (C), PA+ samples contain *P. aeruginosa* (>$10^5$ cells·mL$^{-1}$, red), PA− samples contain catalase+ bacteria different from *P. aeruginosa* (>$10^5$ cells·mL$^{-1}$, green), and MF contains a mixed flora (blue). Negative samples for bacterial infection were determined by a Gram's stain screening test (black). Horizontal bars represent the mean. The dotted line shows signals above two times the standard deviation of the negative samples. *P*-value was obtained using a Kruskall−Wallis test.

developed in our laboratory and schematized in Figure 1B. First, we calibrated the immunosensor with bacterial suspensions of known concentration. In Figures 5A and S8, the signal S increased as the concentration of *P. aeruginosa* increased linearly in the concentration range between $10^4$ and $10^9$ cells·mL$^{-1}$. The limit of detection, expressed as the sample that yields a signal higher than three times the standard deviation of the blank, was $10^5$ cells·mL$^{-1}$, which is the clinical threshold value for respiratory infections. Next, we studied whether the immunosensor was compatible with the sample liquefaction method and whether the matrix could interfere in the detection of *P. aeruginosa*. To test this, a sputum sample from a patient suffering from an infection by *P. aeruginosa* and a sample containing a mixed flora were fractioned and treated with different concentrations of hydrogen peroxide for 60 s. In Figure 5B, samples that were treated only with PBS (0 M $H_2O_2$) could not be differentiated with the immunosensor because bacteria in the sample were still trapped in the matrix, in accordance with our initial hypothesis. As the concentration of $H_2O_2$ increased, the signal S also increased because more antigens were being released from the matrix and the biofilm, in accordance with the results shown in Figures 2 and 3. These results also demonstrate the excellent specificity of our detection kit, which can differentiate an infection by *P. aeruginosa* from a sample containing a mixed flora in a biological matrix as complex as sputum.

To further support this point, a panel of sputum samples that were either positive or negative for infection by *P. aeruginosa*, as well as samples classified as mixed flora, was tested. The method here consisted of a 60 s liquefaction step, followed by immunodetection with mobile biosensors within 7 min. In Figure 5C, all samples classified as a respiratory infection by *P. aeruginosa* yielded a signal two times above the standard deviation of the average value of negative samples. Using this criterion, only one negative sample out of 44 was incorrectly classified as positive. Furthermore, only two out of 32 mixed flora samples yielded a false-positive result. All 16 samples infected with other catalase-producing pathogens were also correctly classified as negative, which demonstrates that higher signals obtained in samples containing *P. aeruginosa* originated from the specific recognition of bacterial antigens, and not from differences in sample liquefaction. The test diagnostic sensitivity (true-positive rate) is 100%, and the specificity (true-negative rate) is 96.7%. While further experiments with a larger cohort of patient samples should be performed to establish the diagnostic sensitivity and specificity, our preliminary results indicate that the proposed method is suitable for the rapid identification of respiratory infections by *P. aeruginosa* at the point of care.

## DISCUSSION

The routine method for treating sputum samples prior to pathogen detection through bacteriological culture involves the addition of dithiothreitol (DTT), which reduces disulfide bonds that cross-link mucins in the matrix. This usually requires adding DTT for at least 30 min in a temperature-controlled bath, followed by sample dispersion with a vortex. In contrast, our enzymatic method generates bubbles that disrupt biofilms (Figures 3, 4, and S4) and liquefy the sample (Figures 2 and S9) within 60 s. The bubbles are generated via the enzymatic conversion of hydrogen peroxide (Figures 2B, S5, and S6), which does not reduce disulfide bonds to a large extent (Figure S7). The proposed method for detecting bacterial biofilms has some notable strengths and limitations compared to the DTT method. For example, our method is more advantageous for point-of-care measurements because it is faster and requires less equipment than the DTT protocol. However, samples that do not contain catalase-producing cells may not be completely liquefied with the $H_2O_2$ method (Figure S9). This is advantageous in the context of *P. aeruginosa* detection because samples that are not liquefied will not release potential interferents. In other words, our method improves the selectivity toward *P. aeruginosa* detection because pathogens that do not produce catalase will remain trapped in the matrix. Another potential limitation is that adding hydrogen peroxide for extended periods of time will kill the cells and therefore these will not grow under standard bacterial culture procedures. However, it could expedite the detection of pathogens when coupled with methods that do not require viable cells, for example, for PCR analysis or immunodetection. Finally, it should be noted that polyclonal antibodies may not be able to distinguish between different bacteria from the *Pseudomonas* genus. However, the prevalence of infections due to bacteria other than *P. aeruginosa* is so low that its impact on clinical diagnosis would be minimum.[37]


https://dx.doi.org/10.1021/acssensors.0c01618
ACS Sens. XXXX, XXX, XXX−XXX

## CONCLUSIONS

In this paper, we introduce a method for disrupting biofilms of *P. aeruginosa* and liquefying respiratory samples in one step. It only requires adding a solution of hydrogen peroxide. The formation of oxygen bubbles by catalase is the key factor for dispersing the matrix and the cells. The release of antigens from the sample allowed us to detect *P. aeruginosa* in sputum samples with a rapid diagnostic test made of paper that utilizes a smartphone as a reader. The whole process, including sample liquefaction and pathogen detection, took less than 8 min. This rapid turnaround time makes the detection kit an ideal method to screen for hospital-acquired respiratory infections that may lead to sepsis.

## ASSOCIATED CONTENT

### Supporting Information

The Supporting Information is available free of charge at https://pubs.acs.org/doi/10.1021/acssensors.0c01618.

Liquefaction of sputum containing *P. aeruginosa* by $H_2O_2$ (Video S1) (MOV).

Liquefaction of sputum containing mixed flora by $H_2O_2$ (Video S2) (MOV).

Inhibition of sputum liquefaction by 0.01 M $NaN_3$ (Video S3) (MOV).

Inhibition of sputum liquefaction by 0.1 M $NaN_3$ (Video S4) (MOV).

Inhibition of sputum liquefaction by 1 M $NaN_3$ (Video S5) (MOV).

Detection of *P. aeruginosa* with ELISA (Figure S1); evaluation of the impact of $H_2O_2$ treatment on antibody−antigen interactions (Figure S2); influence of incubation time with $H_2O_2$ on bacterial antigen release (Figure S3); effect of $H_2O_2$ on the microstructure and cell viability of *P. aeruginosa* biofilms evaluated by CLSM (Figure S4); effect of Fe starvation on bubble production and cell death susceptibility (Figure S5); effect of $H_2O_2$ addition on antigen release and biomass of biofilms grown under Fe starvation conditions (Figure S6); Ellman's reagent reduction by hydrogen peroxide and dithiotreitol (Figure S7); detection of *P. aeruginosa* with immunosensors and a scanner (Figure S8); liquefaction of sputum samples (Figure S9); and comparison between our immunosensor and other methods to detect *P. aeruginosa* (Table S1) (PDF)

## AUTHOR INFORMATION


### Corresponding Authors

**Antonio Clemente** − *Multidisciplinary Sepsis Group, Health Research Institute of the Balearic Islands (IdISBa), 07120 Palma de Mallorca, Spain;* orcid.org/0000-0002-0412-1315; Email: antonio.clemente@ssib.es

**Roberto de la Rica** − *Multidisciplinary Sepsis Group, Health Research Institute of the Balearic Islands (IdISBa), 07120 Palma de Mallorca, Spain;* orcid.org/0000-0002-5750-1469; Email: roberto.delarica@ssib.es

### Authors

**Alejandra Alba-Patiño** − *Multidisciplinary Sepsis Group, Health Research Institute of the Balearic Islands (IdISBa), 07120 Palma de Mallorca, Spain*

**Estrella Rojo-Molinero** − *Servicio de Microbiología, Hospital Son Espases, Health Research Institute of the Balearic Islands (IdISBa), 07120 Palma de Mallorca, Spain*

**Steven M. Russell** − *Multidisciplinary Sepsis Group, Health Research Institute of the Balearic Islands (IdISBa), 07120 Palma de Mallorca, Spain*

**Marcio Borges** − *Multidisciplinary Sepsis Group, Health Research Institute of the Balearic Islands (IdISBa), 07120 Palma de Mallorca, Spain; Multidisciplinary Sepsis Unit, ICU, Son Llàtzer University Hospital,, 07198 Palma de Mallorca, Spain*

**Antonio Oliver** − *Servicio de Microbiología, Hospital Son Espases, Health Research Institute of the Balearic Islands (IdISBa), 07120 Palma de Mallorca, Spain*

Complete contact information is available at: https://pubs.acs.org/10.1021/acssensors.0c01618


### Author Contributions

A.C. and A.A.-P. contributed equally to this work. R.R. and M.B. elaborated the concept. R.R., A.C., and E.R.-M. designed the experiments. A.C., A.A.-P., E.R.-M., and R.R. performed the experiments. S.M.R. developed the app. E.R.-M. and A.O. contributed patient samples. R.R. and A.C. wrote the paper. R.R. and A.O. supervised the project. All authors have given approval to the final version of the manuscript.

### Notes

The authors declare the following competing financial interest(s): R.R., A.C. E.R and A.O. have filed a patent application describing the method for sample liquefaction (P202030403) and patent application PCT/EP2020/075013 describing the method for fabricating paper biosensors.

## ACKNOWLEDGMENTS

R.R. acknowledges financial support through grants FEDER/Ministerio de Ciencia, Innovación y Universidades/Agencia Estatal de Investigación/-Proyecto CTQ2017-82432-R and FEDER/Ministerio de Ciencia, Innovación y Universidades/Agencia Estatal de Investigación/-Proyecto CTQ2017-92226-EXP. R.R. and A.C. aknowledge a Radix and Folium fellowship, respectively, from IdISBa/Impost turisme sostenible/Govern de les Illes Balears. A.A. acknowledges a fellowship for doctoral studies from Roche ("Stop fuga de cerebros" program). We thank J. Piérola (Microscopy Platform, IdISBa) for assistance with imaging experiments.

## REFERENCES

(1) Molinero-Fernández, Á.; Moreno-Guzmán, M.; Arruza, L.; López, M. Á.; Escarpa, A. Toward Early Diagnosis of Late-Onset Sepsis in Preterm Neonates: Dual Magnetoimmunosensor for Simultaneous Procalcitonin and C-Reactive Protein Determination in Diagnosed Clinical Samples. *ACS Sensors* **2019**, *4*, 2117−2123.

(2) Seymour, C. W.; Gesten, F.; Prescott, H. C.; Friedrich, M. E.; Iwashyna, T. J.; Ph, D.; Phillips, G. S.; Lemeshow, S.; Ph, D.; Osborn, T.; et al. Time to Treatment and Mortality during Mandated Emergency Care for Sepsis. *N. Engl. J. Med.* **2017**, *376*, 2235−2244.

(3) Rhodes, A.; Evans, L. E.; Alhazzani, W.; Levy, M. M.; Antonelli, M.; Ferrer, R.; Kumar, A.; Sevransky, J. E.; Sprung, C. L.; Nunnally, M. E.; et al. *Intensive Care Med.* **2017**, *43* (3), 304−377.

(4) Hirsch, E. B.; Tam, V. H. Impact of Multidrug-Resistant Pseudomonas Aeruginosa Infection on Patient Outcomes. *Expert Rev. Pharmacoeconomics Outcomes Res.* **2010**, *10*, 441−451.

(5) Jochumsen, N.; Marvig, R. L.; Damkiær, S.; Jensen, R. L.; Paulander, W.; Molin, S.; Jelsbak, L.; Folkesson, A. The Evolution of Antimicrobial Peptide Resistance in Pseudomonas Aeruginosa Is

Shaped by Strong Epistatic Interactions. *Nat. Commun.* **2016**, *7*, No. 13002.
(6) Jones, R. N. Microbial Etiologies of Hospital-Acquired Bacterial Pneumonia and Ventilator-Associated Bacterial Pneumonia. *Clin. Infect. Dis.* **2010**, *51*, S81−S87.
(7) Amiri, M.; Bezaatpour, A.; Jafari, H.; Boukherroub, R.; Szunerits, S. Electrochemical Methodologies for the Detection of Pathogens. *ACS Sensors* **2018**, *3*, 1059−1086.
(8) Song, J.; Li, Y.; Yin, F.; Zhang, Z.; Ke, D.; Wang, D.; Yuan, Q.; Zhang, X. E. Enhanced Electrochemical Impedance Spectroscopy Analysis of Microbial Biofilms on an Electrochemically in Situ Generated Graphene Interface. *ACS Sensors* **2020**, *5*, 1795−1803.
(9) Zhou, S.; Lu, C.; Li, Y.; Xue, L.; Zhao, C.; Tian, G.; Bao, Y.; Tang, L.; Lin, J.; Zheng, J. Gold Nanobones Enhanced Ultrasensitive Surface-Enhanced Raman Scattering Aptasensor for Detecting Escherichia Coli O157:H7. *ACS Sensors* **2020**, *5*, 588−596.
(10) Zheng, L.; Cai, G.; Qi, W.; Wang, S.; Wang, M.; Lin, J. Optical Biosensor for Rapid Detection of Salmonella Typhimurium Based on Porous Gold@Platinum Nanocatalysts and a 3D Fluidic Chip. *ACS Sensors* **2020**, *5*, 65−72.
(11) Papadakis, G.; Pantazis, A. K.; Ntogka, M.; Parasyris, K.; Theodosi, G. I.; Kaprou, G.; Gizeli, E. 3D-Printed Point-of-Care Platform for Genetic Testing of Infectious Diseases Directly in Human Samples Using Acoustic Sensors and a Smartphone. *ACS Sensors* **2019**, *4*, 1329−1336.
(12) Catala, C.; Mir-Simon, B.; Feng, X.; Cardozo, C.; Pazos-Perez, N.; Pazos, E.; Gómez-de Pedro, S.; Guerrini, L.; Soriano, A.; Vila, J.; et al. Online SERS Quantification of Staphylococcus Aureus and the Application to Diagnostics in Human Fluids. *Adv. Mater. Technol.* **2016**, *1*, No. 11600163.
(13) Pazos-Perez, N.; Pazos, E.; Catala, C.; Mir-Simon, B.; Gomez-De Pedro, S.; Sagales, J.; Villanueva, C.; Vila, J.; Soriano, A.; Garcia De Abajo, F. J.; et al. Ultrasensitive Multiplex Optical Quantification of Bacteria in Large Samples of Biofluids. *Sci. Rep.* **2016**, *6*, No. 29014.
(14) Dong, T.; Santos, S.; Yang, Z.; Yang, S.; Kirkhus, N. E. Sputum and Salivary Protein Biomarkers and Point-of-Care Biosensors for the Management of COPD. *Analyst* **2020**, *145*, 1583−1604.
(15) Li, X.; Kong, H.; Mout, R.; Saha, K.; Moyano, D. F.; Robinson, S. M.; Rana, S.; Zhang, X.; Riley, M. A.; Rotello, V. M. Rapid Identification of Bacterial Biofilms and Biofilm Wound Models Using a Multichannel Nanosensor. *ACS Nano* **2014**, *8*, 12014−12019.
(16) Passos da Silva, D.; Matwichuk, M. L.; Townsend, D. O.; Reichhardt, C.; Lamba, D.; Wozniak, D. J.; Parsek, M. R. The Pseudomonas Aeruginosa Lectin LecB Binds to the Exopolysaccharide Psl and Stabilizes the Biofilm Matrix. *Nat. Commun.* **2019**, *10*, No. 2183.
(17) Kukhtin, A. V.; Norville, R.; Bueno, A.; Qu, P.; Parrish, N.; Murray, M.; Chandler, D. P.; Holmberg, R. C.; Cooney, C. G. A Benchtop Automated Sputum-to-Genotype System Using a Lab-on-a-Film Assembly for Detection of Multidrug-Resistant Mycobacterium Tuberculosis. *Anal. Chem.* **2020**, *92*, 5311−5318.
(18) Massai, F.; Imperi, F.; Quattrucci, S.; Zennaro, E.; Visca, P.; Leoni, L. A Multitask Biosensor for Micro-Volumetric Detection of N-3-Oxo-Dodecanoyl-Homoserine Lactone Quorum Sensing Signal. *Biosens. Bioelectron.* **2011**, *26*, 3444−3449.
(19) Kim, J. H.; Yeo, W. H.; Shu, Z.; Soelberg, S. D.; Inoue, S.; Kalyanasundaram, D.; Ludwig, J.; Furlong, C. E.; Riley, J. J.; Weigel, K. M.; et al. Immunosensor towards Low-Cost, Rapid Diagnosis of Tuberculosis. *Lab Chip* **2012**, *12*, 1437−1440.
(20) Inoue, S.; Becker, A. L.; Kim, J. H.; Shu, Z.; Soelberg, S. D.; Weigel, K. M.; Hiraiwa, M.; Cairns, A.; Lee, H. B.; Furlong, C. E.; et al. Semi-Automated, Occupationally Safe Immunofluorescence Microtip Sensor for Rapid Detection of Mycobacterium Cells in Sputum. *PLoS One* **2014**, *9*, 1−7.
(21) Hiraiwa, M.; Kim, J.; Lee, H.; Inoue, S.; Becker, A. L.; Weigel, K. M.; Cangelosi, G. A.; Lee, K.; Chung, J. Amperometric Immunosensor for Rapid Detection of Mycobacterium Tuberculosis. *J. Micromech. Microeng.* **2015**, *25*, No. 05501.
(22) Pastells, C.; Pascual, N.; Sanchez-Baeza, F.; Marco, M. P. Immunochemical Determination of Pyocyanin and 1-Hydroxyphenazine as Potential Biomarkers of Pseudomonas Aeruginosa Infections. *Anal. Chem.* **2016**, *88*, 1631−1638.
(23) Huang, X.; Chen, R.; Xu, H.; Lai, W.; Xiong, Y. Nanospherical Brush as Catalase Container for Enhancing the Detection Sensitivity of Competitive Plasmonic ELISA. *Anal. Chem.* **2016**, *88*, 1951−1958.
(24) Jiang, X.; Jin, H.; Sun, Y.; Sun, Z.; Gui, R. Assembly of Black Phosphorus Quantum Dots-Doped MOF and Silver Nanoclusters as a Versatile Enzyme-Catalyzed Biosensor for Solution, Flexible Substrate and Latent Fingerprint Visual Detection of Baicalin. *Biosens. Bioelectron.* **2020**, *152*, No. 112012.
(25) Zheng, L.; Cai, G.; Wang, S.; Liao, M.; Li, Y.; Lin, J. A Microfluidic Colorimetric Biosensor for Rapid Detection of Escherichia Coli O157:H7 Using Gold Nanoparticle Aggregation and Smart Phone Imaging. *Biosens. Bioelectron.* **2019**, *124*−*125*, 143−149.
(26) Xie, Y.; Fu, S.; Wu, J.; Lei, J.; Ju, H. Motor-Based Microprobe Powered by Bio-Assembled Catalase for Motion Detection of DNA. *Biosens. Bioelectron.* **2017**, *87*, 31−37.
(27) Russell, S. M.; Alba-Patiño, A.; Borges, M.; de la Rica, R. Multifunctional Motion-to-Color Janus Transducers for the Rapid Detection of Sepsis Biomarkers in Whole Blood. *Biosens. Bioelectron.* **2019**, *140*, No. 111346.
(28) Sun, J.; Mathesh, M.; Li, W.; Wilson, D. A. Enzyme-Powered Nanomotors with Controlled Size for Biomedical Applications. *ACS Nano* **2019**, *13*, 10191−10200.
(29) Lamberg, P.; Shleev, S.; Ludwig, R.; Arnebrant, T.; Ruzgas, T. Performance of Enzymatic Fuel Cell in Cell Culture. *Biosens. Bioelectron.* **2014**, *55*, 168−173.
(30) Song, G.; Chen, Y.; Liang, C.; Yi, X.; Liu, J.; Sun, X.; Shen, S.; Yang, K.; Liu, Z. Catalase-Loaded TaOx Nanoshells as Bio-Nanoreactors Combining High-Z Element and Enzyme Delivery for Enhancing Radiotherapy. *Adv. Mater.* **2016**, *28*, 7143−7148.
(31) Alba-Patiño, A.; Russell, S. M.; Borges, M.; Pazos-Perez, N.; Alvarez-Puebla, R. A.; de la Rica, R. Nanoparticle-Based Mobile Biosensors for the Rapid Detection of Sepsis Biomarkers in Whole Blood. *Nanoscale Adv.* **2020**, *2*, 1253−1260.
(32) Alba-Patiño, A.; Adrover-Jaume, C.; de la Rica, R. Nanoparticle Reservoirs for Paper-Only Immunosensors. *ACS Sensors* **2020**, *5*, 147−153.
(33) Jordana-Lluch, E.; Garcia, V.; Kingdon, A. D. H.; Singh, N.; Alexander, C.; Williams, P.; Hardie, K. R. A Simple Polymicrobial Biofilm Keratinocyte Colonization Model for Exploring Interactions Between Commensals, Pathogens and Antimicrobials. *Front. Microbiol.* **2020**, *11*, No. 291.
(34) Mangwani, N.; Shukla, S. K.; Kumari, S.; Das, S.; Toleti, S. R. Effect of biofilm parameters and extracellular polymeric substances composition on polycyclic aromatic hydrocarbons degradation. *RSC Adv.* **2016**, *6*, 57540−57551.
(35) Frederick, J. R.; Elkins, J. G.; Bollinger, N.; Hasset, D. J.; McDermott, T. R. Factors affecting catalase expression in Pseudomonas aeruginosa biofilms and planktonic cells. *Appl. Environ. Microbiol.* **2001**, *67*, 1375−1379.
(36) Sultana, S. T.; Call, D. R.; Beyenal, H. Eradication of Pseudomonas Aeruginosa Biofilms and Persister Cells Using an Electrochemical Scaffold and Enhanced Antibiotic Susceptibility/692/700/631/1647 Article. *npj Biofilms Microbiomes* **2016**, *2*, 2.
(37) Fernández, M.; Porcel, M.; de la Torre, J.; Molina-Henares, M. A.; Daddaoua, A.; Llamas, M. A.; Roca, A.; Carriel, V.; Garzon, I.; Ramos, J. L.; Alaminos, M.; Duque, E. Analysis of the pathogenic potential of nosocomial Pseudomonas putida strains. *Front. Microbiol.* **2015**, *6*, 871.


https://dx.doi.org/10.1021/acssensors.0c01618
ACS Sens. XXXX, XXX, XXX−XXX